Effect of intake air temperature and air-fuel ratio on particulates in gasoline and n-butanolfueled homogeneous charge compression ignition engine

2 authors, including:

Avinash Kumar Agarwal
Indian Institute of Technology Kanpur
582 PUBLICATIONS **23,244** CITATIONS

Effect of intake air temperature and air–fuel ratio on particulates in gasoline and n-butanolfueled homogeneous charge compression ignition engine

Rakesh K Maurya and Avinash K Agarwal

Published by:

$SAGE

http://www.sagepublications.com

On behalf of:

Institution of
**MECHANICAL
ENGINEERS**

Institution of Mechanical Engineers

Additional services and information for *International Journal of Engine Research* can be found at:

Email Alerts: http://jer.sagepub.com/cgi/alerts

Subscriptions: http://jer.sagepub.com/subscriptions

Reprints: http://www.sagepub.com/journalsReprints.nav

Permissions: http://www.sagepub.com/journalsPermissions.nav

Citations: http://jer.sagepub.com/content/15/7/789.refs.html

>> Version of Record - Aug 19, 2014

OnlineFirst Version of Record - Feb 4, 2014

What is This?

Effect of intake air temperature and air–fuel ratio on particulates in gasoline and n-butanolfueled homogeneous charge compression ignition engine

Rakesh K Maurya[1,2] and Avinash K Agarwal[1]

Abstract

An experimental study was conducted to investigate the effect of engine operating parameters on exhaust particulate size–number distribution in a homogeneous charge compression ignition engine fueled with gasoline and n-butanol. In this investigation, portfuel injection was done for preparing homogeneous charge, and intake air preheating was used for auto-ignition of the charge. Engine exhaust particle sizer was used for measuring size–number distribution of particulate matter emitted from the homogeneous charge compression ignition engine. Experiments were conducted at different engine speeds by varying intake air temperature and air–fuel ratio of the charge. Effect of engine operating parameters on particulate size–number distribution, size–surface area distribution, and total particulate number concentration was investigated. Most significant particle numbers were in the range of 6–150 nm mobility diameter for all test conditions. n-Butanol showed relatively higher peak number concentration and lower mobility diameter corresponding to the peak concentrations as compared to baseline gasoline. On increasing intake air temperature, mobility diameters corresponding to peak number concentration of particles moved towards lower mobility diameters. Count mean diameter of particles was in the range of 35–80 nm and 20–65 nm for gasoline and n-butanol, respectively, for all test conditions in homogeneous charge compression ignition operating range.

Introduction

Homogeneous charge compression ignition (HCCI) is an extremely promising combustion concept currently being explored as an alternative to conventional engine combustion modes for higher efficiency and extremely low NO_x and particulate emissions. HCCI means that the fuel and air should be mixed homogeneously before the start of combustion, and the mixture is auto-ignited due to increase in temperature at the end of compression stroke. However, precisely controlling the combustion is a key for improved performance in terms of efficiency and emissions. In HCCI engine, combustion is completely controlled by chemical kinetics and is therefore affected by variables such as fuel composition, equivalence ratio, and thermodynamic state of air–fuel mixture.[1] HCCI engines are inherently fuel-flexible theoretically and can potentially operate on low- or high-

grade fuels, as long as the fuel can be heated to the point of auto-ignition toward the end of compression stroke[2]. In particular, HCCI engines can be fueled with variety of alcohols.[3–7] HCCI engine with n-butanol as a renewable fuel offers a promising solution to tackle some of the major challenges before full realization of "green powertrains." Butanol is a competitive alcohol

[1]Engine Research Laboratory, Department of Mechanical Engineering, Indian Institute of Technology Kanpur, Kanpur, India
[2]School of Mechanical, Materials and Energy Engineering, Indian Institute of Technology Ropar, Rupnagar, India

Corresponding author:
Avinash K Agarwal, Engine Research Laboratory, Department of Mechanical Engineering, Indian Institute of Technology Kanpur, Kanpur 208016, India.
Email: akag@iitk.ac.in

fuel, which can potentially be produced by fermentation of various organic residues, including waste products from industrial processes.[8] Butanol is a good biofuel for internal combustion (IC) engines and can be used in spark ignition (SI) engines[9–11] as well as compression ignition (CI) engines[12–15] in blended or pure form. Rakopoulos et al. found that butanol–diesel blends had a slightly higher specific fuel consumption due to its relatively lower heating value, but they reported a slight higher brake thermal efficiency. NO_x emissions reduced slightly, but the smoke reduced significantly for butanol–diesel blends.[14,15] These studies demonstrated that butanol can be used advantageously and safely as a admixture with diesel in CI engines.[12–15] Butanol has relatively higher calorific value compared to ethanol or methanol, and it also does not absorb moisture from the atmospheric air. Very few fundamental studies are conducted to investigate combustion characteristics of butanol.[16–18] Agathou and Kyritsis[17] found that butanol nonpremixed flames can sustain higher strain rates at extinction than the corresponding flames of ethanol, which is currently used as a biofuel. Liu et al.[18] found that butanol had a higher potential thermal efficiency, lower flame luminosity, and soot emissions compared to soybean biodiesel. Butanol has four isomers: 1-butanol (or n-butanol), 2-butanol, iso-butanol, and tert-butanol. However, out of these four, only the first three are biologically produced in nature.[19] Mitsingas and Kyritsis[19,20] reported that even though all isomers share essentially the same adiabatic flame temperature, n-butanol flames could sustain a consistently higher extinction strain rate than the flames of other isomers (iso-butanol and sec-butanol). Fushimi et al.[21] reported that n-butanol is best for gas–oil blending use among the three isomers. Considering these advantages of n-butanol and HCCI engines, it was chosen to explore the combined advantages of HCCI combustion with oxygenated biofuels (n-butanol) and compare it with baseline gasoline HCCI.

Several adverse health effects are associated with the ultra-fine particles (diameter < 100 nm) emitted in the engine exhaust. Researchers have shown that fine particulates can penetrate the cell membrane, enter into the blood stream, and reach the brain to cause mutagenic effects.[22,23] Therefore, measurement and control of engine particulates is extremely important for the engine researchers and automotive manufacturers. Few studies reported the effect of various engine operating conditions on particulate emission in HCCI engines.[24–29] Price et al.[24] found that particulate matter (PM) emissions in HCCI combustion are non-negligible, and significant concentration of accumulation mode particulates was detected. Kittelson and Franklin[25] suggested that carbonaceous agglomerates, which comprise most of the PM mass, are significantly lower in HCCI engines. In HCCI combustion, PM emissions comprise lesser solid carbon accumulation mode particles and more volatile particles in the nuclei mode.

All studies mentioned above lead us to the conclusion that the thermal conditions prevailing inside the combustion chamber and the fuel injection timings, at which HCCI engine is operated, affect emissions, including PM emissions. Particulate emission data for port fuel–injected HCCI combustion for butanol are not available in the open literature; therefore, it is worth investigating the effect of engine operating conditions on PM emissions from n-butanol-fueled HCCI engine at different engine speeds vis-à-vis baseline gasoline-fueled HCCI engine.

Experimental setup

Our previous article[26] covers detailed explanation of the experimental setup; therefore, in this section, only brief description of the engine setup and experimental procedure is provided. A four-cylinder diesel engine was modified, and HCCI combustion was achieved in one of the four cylinders. Experimental observations for this study were made on this HCCI cylinder. Technical specifications of the unmodified test engine are provided in Table 1. Intake and exhaust manifolds of HCCI cylinder were separated from the remaining three cylinders. Schematic of the experimental setup is shown in Figure 1.

Table 1. Test engine specifications.

Make/model	Mahindra/load-king
No. of cylinders	Four
Displaced volume	652 cc/cylinder
Stroke/bore	94/94 mm
Connecting rod length	158 mm
Compression ratio	17.5:1
Number of valves	2/cylinder
Exhaust valve open/close	56° BBDC/5° ATDC
Inlet valve open/close	10° BTDC/18° ABDC

BBDC: before bottom dead center; ABDC: after bottom dead center; BTDC: before top dead center; ATDC: after top dead center.

1. Hot-film Air Mass Meter 2. Air Pre-heater 3. Solenoid Fuel Injector 4. Rotary Shaft Encoder 5. Piezoelectric Pressure Transducer 6. Exhaust Plenum 7. Emission Analyzer 8.Fuel Pump 9.Compact RIO 10. Charge Amplifier 11. Driver Circuit 12. Computer 13. Eddy Current Dynamometer 14. Engine 15.Thermo-diluter 16. EEPS
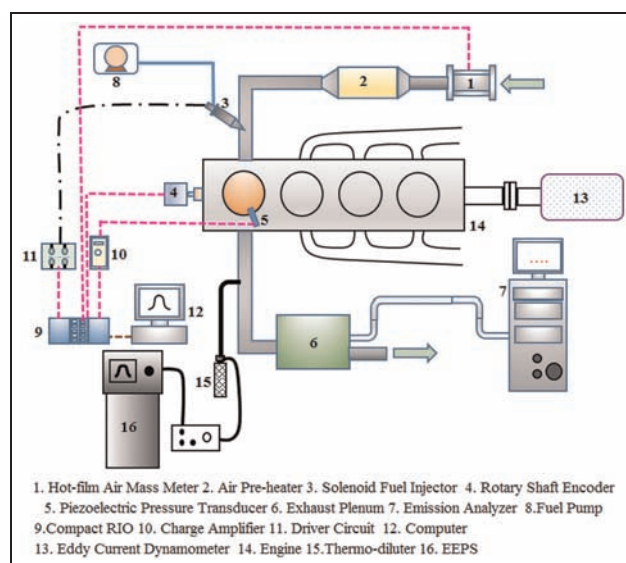
Figure 1. Schematic of the experimental setup.
EEPS: engine exhaust particle sizer.

Test fuel was premixed with air using port fuel injector installed in the intake manifold. Electronic fuel injector had four nozzle holes, and the fuel was injected in the intake manifold at 3 bar fuel injection pressure. The quantity of fuel injected in every cycle and injection timings were controlled using a micro-controller (CompactRIO-9014; National Instruments) and a customized injection driver circuit. CompactRIO micro-controller was programmed by LabVIEW FPGA and LabVIEW Real-Time module software. The CompactRIO micro-controller receives signals from precision shaft encoder (H25D-SS-2160-ABZC; BEI), air mass flow meter (HFM5; Bosch), and an in-cylinder piezoelectric pressure transducer (6013; Kistler). CompactRIO generates an output pulse to trigger the fuel injector after processing the acquired signals, according to the user-defined operating conditions. Based on the output pulse, fuel injector injects the required quantity of fuel in the intake manifold, at an appropriate time.

Air supplied to HCCI cylinder was measured by a hot-film air mass flow meter, which precisely measured the actual intake air mass flow rate. To achieve HCCI combustion with proper combustion phasing of gasoline like fuels, the air–fuel mixture was preheated to a required temperature before entering the cylinder. Fresh air entering the engine was preheated using an electric air preheater, installed upstream of the intake manifold. The intake air preheater was controlled by a closed-loop controller, which maintained constant intake air temperature, as defined by the user. The heater controller took feedback from a thermocouple installed in the intake manifold, immediately upstream of the fuel injector. A thermocouple in conjunction with a digital temperature indicator was used for measurement of intake and exhaust gas temperatures. The in-cylinder pressure was measured using a piezoelectric pressure transducer, which was mounted flush with the cylinder head. To measure the crank angle degree (CAD) position, a precision optical shaft encoder was coupled on the crankshaft. The in-cylinder pressure data acquisition and combustion analysis were done using a LabVIEW-based program developed for this study.

In this study, engine exhaust particle sizer (EEPS) was used to measure the particulate size–number distribution in the engine exhaust. The EEPS spectrometer is a fast-response, high-resolution instrument, which measures particle number concentrations in the diluted engine exhaust. EEPS spectrometer provides both high temporal resolution and reasonable size resolution by using the same basic technique as that of a scanning mobility particle sizer (SMPS) system albeit with multiple detectors working in parallel. The EEPS is designed specifically to measure particulates emitted from engines and vehicles. It measures particles with sizes ranging from 5.6 to 560 nm with a size resolution of 16 channels per decade (a total of 32 channels). The electrometers are read at 10 Hz frequency by a microprocessor, which then inverts the current/charge data to particle size and number distribution.[30] The instrument draws in a sample of the exhaust flow continuously. Rotating disk thermo-diluter was required for diluting and preconditioning the exhaust gas sample, located upstream of EEPS (Figure 1). A portion of raw exhaust was mixed with the heated and filtered air in the disk cavity of the thermo-diluter. Thermo-diluter draws exhaust gas sample directly from the exhaust line using a sampling probe. Sampling probe was designed in such a manner that the particle losses due to nonisokinetic sampling were negligible, therefore can be neglected. Exhaust gas sampling was done at a dilution ratio of 114:1 in the present investigation.

Results and discussion

In this section, the experimental results of particulate emissions from HCCI engine fueled with gasoline and n-butanol at different engine operating conditions are presented. Measurement of particulate size distribution was done after the engine was thermally stabilized for each test point. Sampling was done for 1 min at a sampling frequency of 1 Hz, and the results presented are an average of these 60 data points collected at each test point. Measurement at each test point was repeated twice in order to ensure repeatability of the data. Results are presented in the form of particulate number–size distribution in the exhaust per unit volume (after accounting for the dilution factor).

Experiments were conducted at different intake air temperatures and relative air–fuel ratios (λ) using n-butanol and baseline gasoline at 1200 and 2400 r/min. Figures 2 and 3 show the HCCI operating range for baseline gasoline and n-butanol, respectively. The HCCI operating region was determined by operating limits of high- and low-load boundaries, which were defined by engine knock and combustion stability. In this study, ringing intensity (RI) was used as a criterion to define high-load limit. Fluctuations in the indicated mean effective pressure (IMEP) was used as a measure of combustion stability and expressed as COV_{IMEP}. The coefficient of variation (COV) of IMEP was calculated from the data of 2000 consecutive engine cycles and was used to define the low-load HCCI limit (misfire boundary). In this study, acceptable higher and lower boundary values were taken as RI < 6 MW/m^2 and COV_{IMEP} < 3.5%. The values of RI and COV_{IMEP} used were taken from published literature for similar displacement engines.[31,32]

Figures 2 and 3 show HCCI operating range obtained by applying high- and low-load limit criterion for gasoline and n-butanol at 1200 and 2400 r/min. In Figures 2 and 3, contour lines represent the constant IMEP lines. Figure 2 shows that IMEP contours are more horizontally inclined for both test fuel at the two speeds. This observation indicates that IMEP (contour lines) was largely affected by λ in HCCI operating
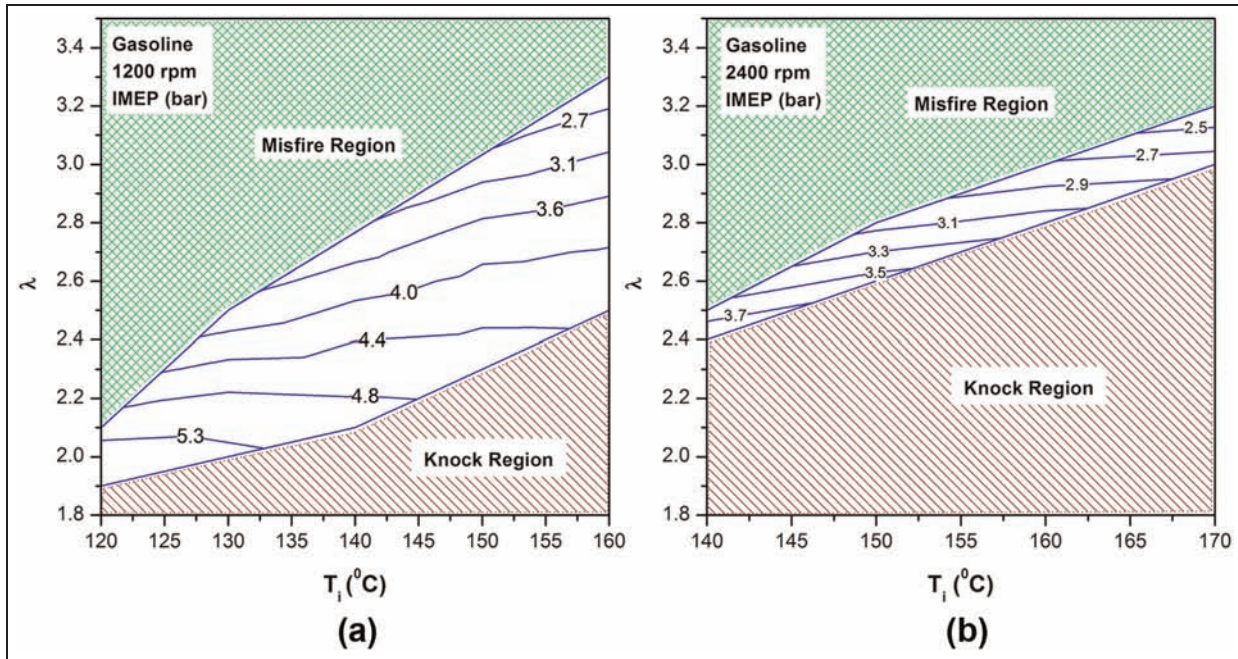
Figure 2. HCCI operating range for gasoline at (a) 1200 and (b) 2400 r/min.
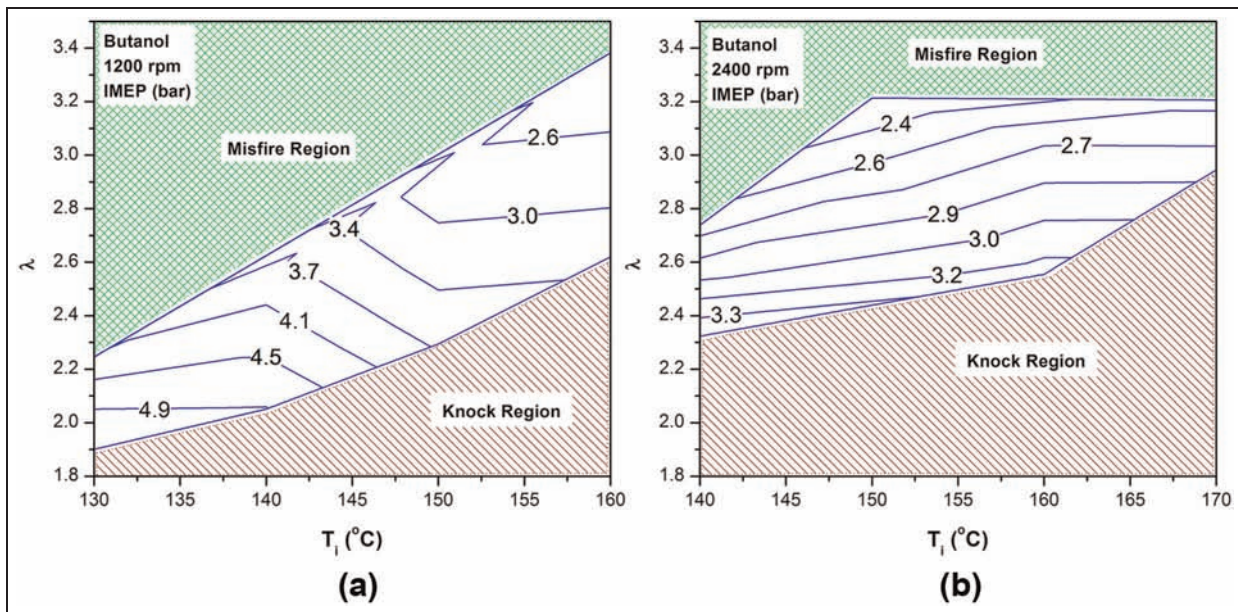IMEP: indicated mean effective pressure.

Figure 3. HCCI operating range for n-butanol at (a) 1200 and (b) 2400 r/min.
IMEP: indicated mean effective pressure.

region. Intake air temperature affected mainly the combustion phasing, which had a weak effect on IMEP in HCCI operating region, defined by high- and low-load limit, as discussed above. It was obvious that the engine output in the HCCI operating range was determined by λ, since the richer mixture (higher energy input) led to higher power output. It can be noted from Figures 2 and 3 that IMEP decreased as engine operated on leaner mixture and IMEP increased as engine operating point moved closer to richer mixture and lower intake

air temperatures. It can also be noted from Figures 2 and 3 that operating region area decreased with increasing engine speed for both test fuels. Minimum λ (richest mixture) in HCCI operating range increased (mixture becomes leaner) for each fuel with increasing engine speed. Therefore, higher load boundary decreased as engine speed increased, due to lower energy input (leaner mixture).

Figures 4 and 5 show the particle size–number distribution for gasoline and butanol at 1200 and 2400 r/min
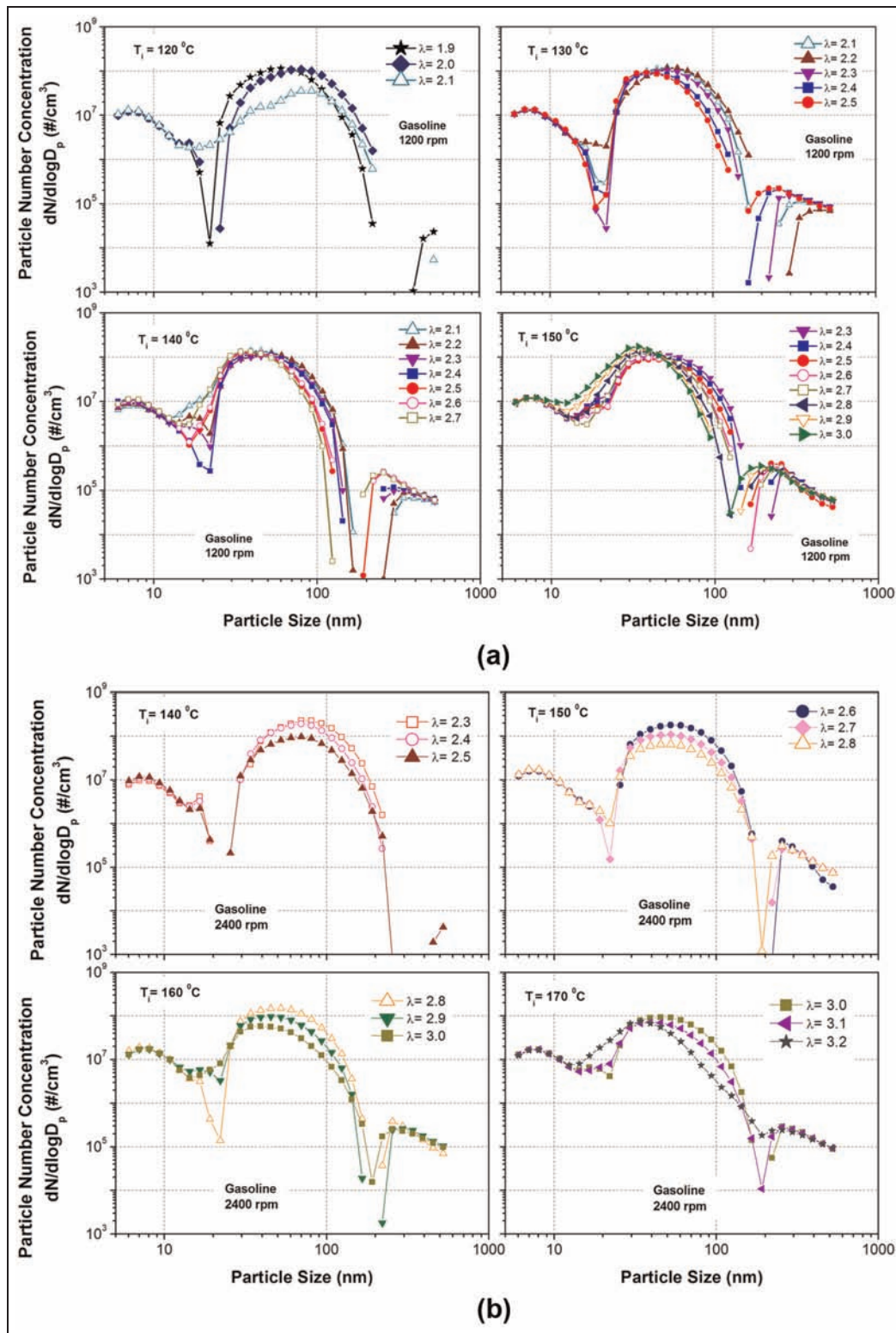
Figure 4. Particle size–number distributions for gasoline HCCI combustion with varying intake temperatures and λ at (a) 1200 and (b) 2400 r/min.

with varying intake air temperature and λ. It is observed from Figures 4 and 5 that particle numbers increased as engine was operated using richer mixtures at each intake air temperature for both fuels. Peak concentration of particles depends on the mixture strength (i.e. engine load) and intake air temperature

(i.e. combustion phasing) for both fuels. It can be observed from Figures 4 and 5 that peak number concentration of gasoline particulates was between 3.56×10^7 and 1.75×10^8 particles/cm^3 at 1200 r/min and 5.75×10^7 and 2.30×10^8 particles/cm^3 at 2400 r/min. Peak number concentration of n-butanol particulates
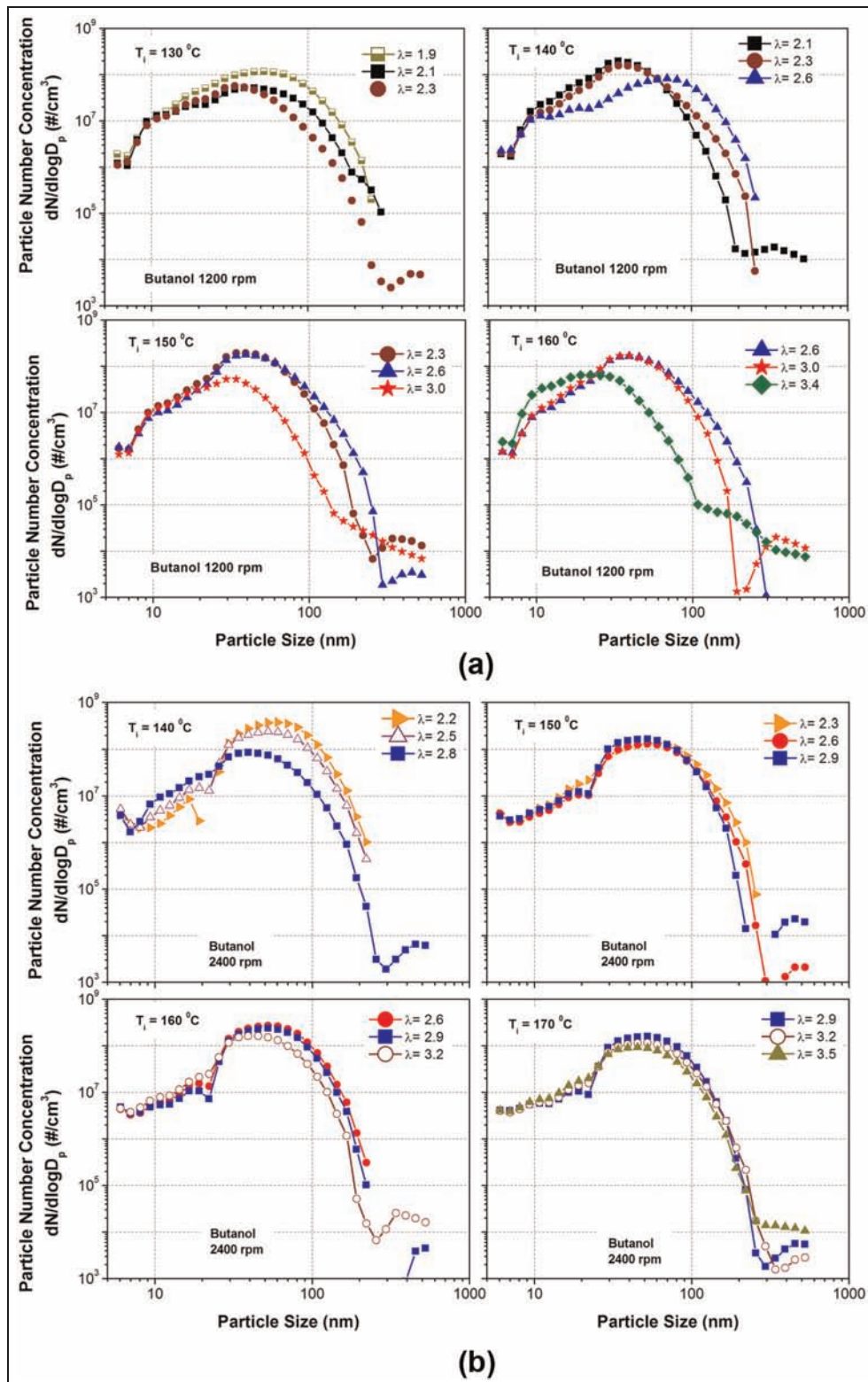
Figure 5. Particle size–number distributions for n-butanol HCCI combustion with varying intake temperatures and λ at (a) 1200 and (b) 2400 r/min.

was between 5.14×10^7 and 1.96×10^8 particles/cm³ at 1200 r/min and 8.57×10^7 and 3.85×10^8 particles/ cm³ at 2400 r/min. Maximum peak concentration was higher at higher engine speeds for both fuels. n-Butanol had higher peak concentration at both engine speeds compared to baseline gasoline. For all test conditions,

particle sizes having significant number of particles were in the range of 6–150 nm.

Price et al.[24] discussed various reasons for non-negligible PM emissions from direct injection (DI)-HCCI gasoline engines. Various factors affecting the PM emissions from HCCI engines suggested by them
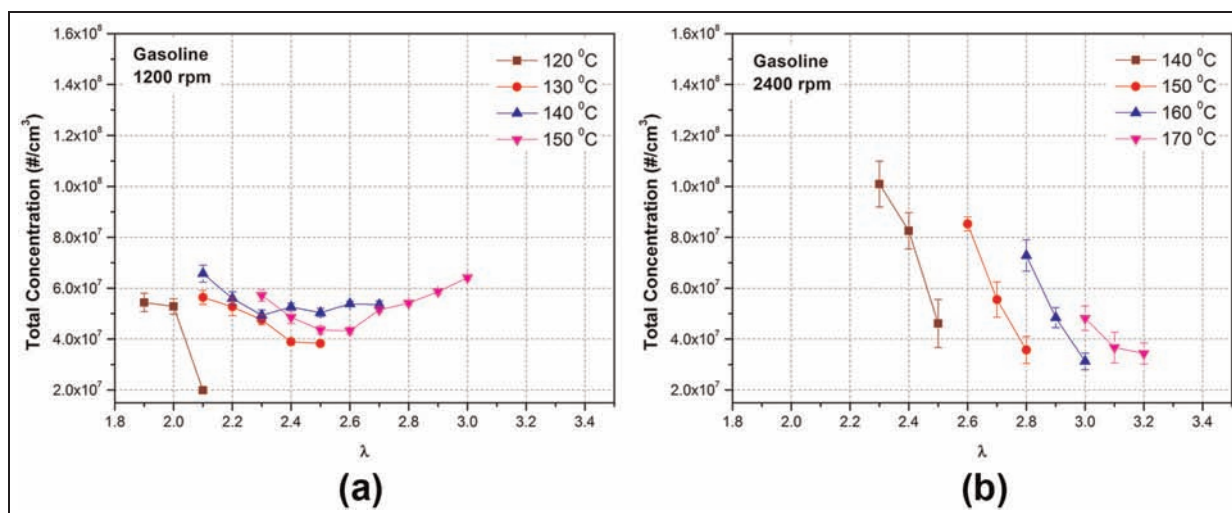
Figure 6. Variation of total number concentration of particles at (a) 1200 and (b) 2400 r/min for gasoline.

were piston and wall wetting, charge heterogeneity, condensation, nucleation, ash, and trace metal emissions. Condensable PM fraction was expected to be significant in HCCI mode for two reasons. First, high unburned gas phase hydrocarbon (HC) emissions due to lower combustion temperature in HCCI mode leading to higher particulate phase HC. Second, temperature in the expansion stroke was not adequate to oxidize all unburnt HCs that diffused out of the crevice volume. Some of these HCs remain suspended in the exhaust and eventually condense, when temperatures become low enough.[24]

It can be observed from Figures 4 and 5 that leaner mixtures show the peak concentration for lower mobility diameters at each intake air temperature for both fuels. It was found that mobility diameters were in the range of 22–52 and 39–60 nm at 1200 and 2400 r/min, respectively, for peak particle number concentrations using n-butanol. While for gasoline, mobility diameters were in the size range of 34–80 nm corresponding to peak particle number concentration at both test speeds, which were comparatively larger than n-butanol. This observation indicated that particles from n-butanol HCCI were smaller as compared to baseline gasoline HCCI. Mobility diameters with peak concentration in gasoline HCCI were also larger compared to gasoline SI engine (typically < 25 nm).[33] It was also observed that the mobility diameters corresponding to peak concentration of particles shifted toward lower mobility diameters with increasing intake air temperatures.

Figures 4 and 5 show that particulate size–number distribution curves for gasoline showed different behaviors in particle size range less than 20 nm. Particle number concentrations in the size range close to 10 nm had number concentration of the order of 10^6 particles/ cm^3 for n-butanol. Gasoline HCCI particles in the size range of 10 nm had number concentration of the order 10^7 particles/cm^3, which was an order of magnitude higher as compared to n-butanol (Figures 4 and 5). On

increasing intake air temperature, nuclei mode particles increased for both fuels.

Franklin[34] demonstrated that almost all particles measured in ethanol HCCI combustion with different control strategies were volatile with no measureable concentration of solid accumulation mode particles. In the absence of solid nucleation mode particles, which acted as adsorption sites, only gas-to-particle conversion processes were available to the organic vapors in the exhaust as it got diluted and cooled, leading to homogeneous nucleation and condensation. This led to formation of volatile, nucleation mode particles. It was reported that in conventional CI engines, composition of volatile nucleation mode particles shifted toward characteristics dominated by lubricating oil origin particles with increasing engine load.[35] This study suggested that higher in-cylinder temperatures may lead to formation of higher lubricating oil–related nucleation mode particles. In this study, size–number distribution of particulates increased at higher load (richer mixture), which was due to higher in-cylinder temperatures as compared to lower loads (leaner mixtures) (Figures 4 and 5). Sakurai et al.[36] also reported that the volatile PM was composed of at least 95% compounds originating from unburned lubricating oil at light to moderate loads in diesel engines. HCCI engines use similar configuration of lubricating system, piston, and piston rings as CI engines. Therefore, delivery of lubricating oil to the combustion chamber and associated processes in the combustion chamber may be similar.[34] Additionally, total hydrocarbon (THC) emissions decrease at higher intake air temperatures, while particle numbers increase (Figures 4–7). In one study, it was reported for a hydrogen SI engine that with increasing in-cylinder temperature, organic carbon levels of the PM also increased.[37] This was reportedly because of higher degree of breakdown of the lubricating oil film present on the cylinder walls. Similar phenomenon may also take place in HCCI engines, and upon increasing
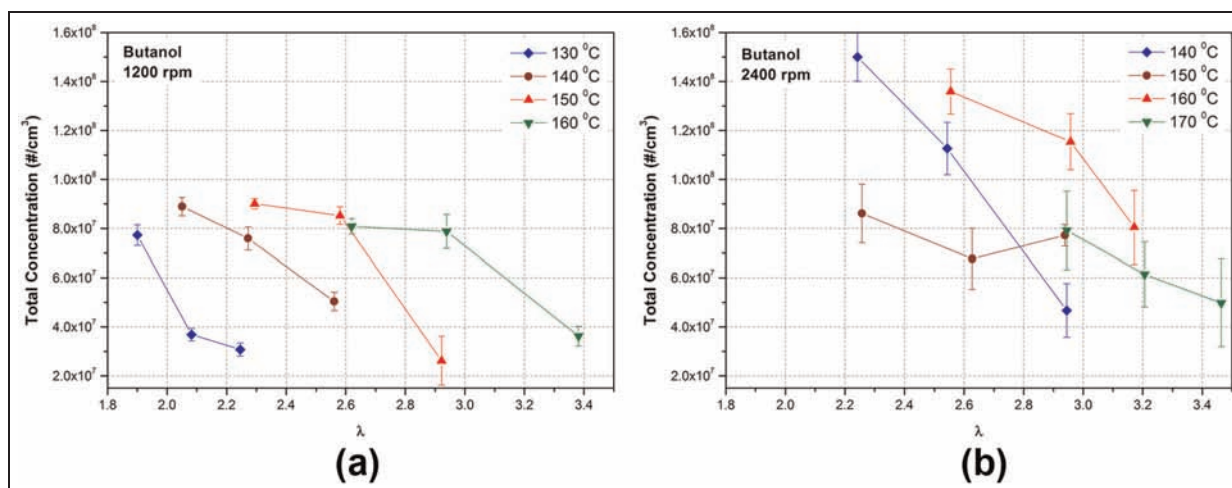
Figure 7. Variation of total number concentration of particles at (a) 1200 and (b) 2400 r/min for n-butanol.
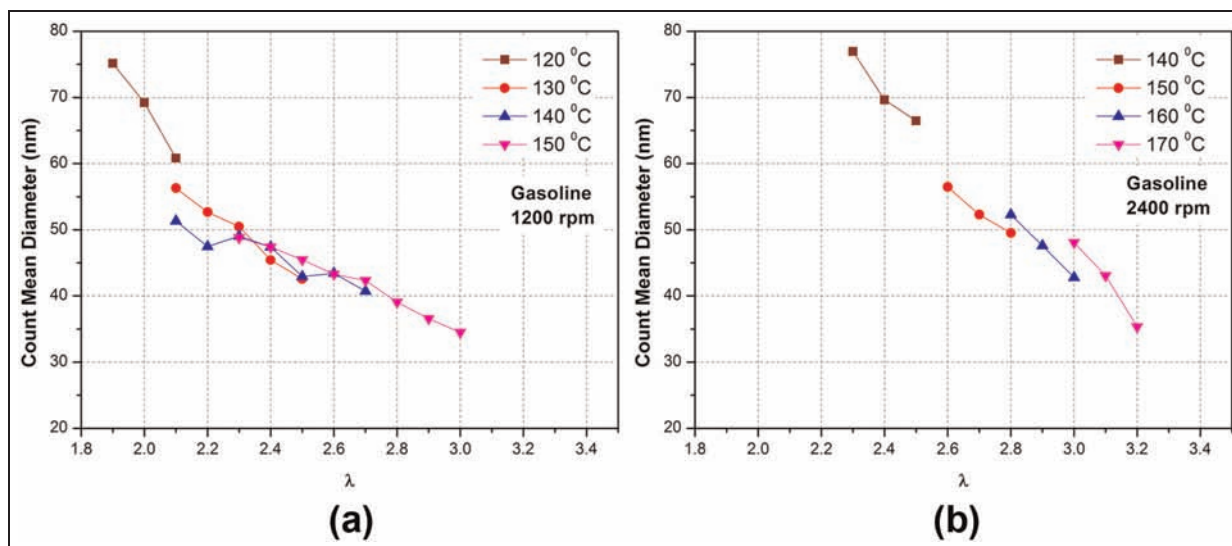

Figure 8. Count mean diameter of particles for baseline gasoline at (a) 1200 and (b) 2400 r/min.

intake air temperature, rate of pressure rise might increase rapidly in HCCI engines.

Figures 6 and 7 show the total number concentration of particles at different λ and T_i for gasoline and n-butanol at 1200 and 2400 r/min. It can be noted from these figures that as mixture becomes leaner, total particle concentration decreased for all test conditions except (T_i = 140 °C and 150 °C) for gasoline at 1200 r/ min. This suggests that on increasing the fueling (load), total particle concentration increased and the trend agrees with the observations made for engines using conventional combustion modes.[33] Total concentration of particles increased with increasing intake air temperature for constant fueling, which was possibly due to increase in nuclei mode particles at higher temperature. Maximum value to total particulate concentration was lower for gasoline compared to n-butanol at both engine speeds. The total concentration of particles was higher for richer mixture conditions and comparable

for leaner conditions, as compared to a gasoline HCCI study.[27] It can also be noted from Figures 6 and 7 that maximum total concentration of particles increased at higher engine speeds for both fuels.

Average particle size is represented by count mean diameter (CMD), which provides a basis for comparing overall size of the emitted particulates for different engine operating conditions. Figures 8 and 9 show variation of CMD of particulates with varying intake air temperatures and λ for gasoline and n-butanol, respectively, at 1200 and 2400 r/min.

CMD of particulates was in the range of 35–80 nm for gasoline under all test conditions in HCCI operating range. However, for n-butanol, it was in the range of 20–65 nm under identical HCCI operating range. This observation indicated that the average diameter of particles emitted from n-butanol was smaller compared to baseline gasoline. Smaller molecular chain length of n-butanol possibly contributes to smaller CMD of
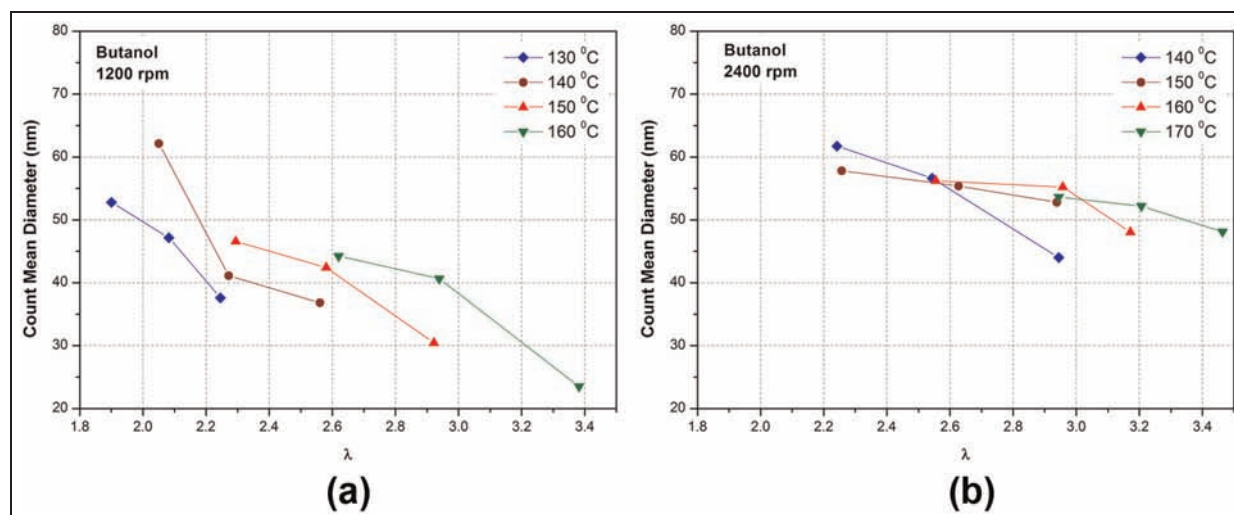
Figure 9. Count mean diameter of particles for n-butanol at (a) 1200 and (b) 2400 r/min.

particulates. Lower CMD indicates lower concentration of accumulation mode particles and/or higher concentration of nuclei mode particles for n-butanol in comparison to baseline gasoline. It can also be noted from Figures 9 and 10 that at any intake air temperature, CMD increased for richer mixtures and decreased as mixture becomes leaner for both fuels at all engine speeds.

The surface area versus size distribution is very important from toxicology point of view. Particulate surface area distribution is an indicator of effectiveness of interaction of particulates with the respiratory system, and it determines their effect on human health. Higher the particulate surface area, higher will be the possibility of surface adsorption of the polycyclic aromatic hydrocarbons (PAHs) leading to higher toxic potential.[33] Smaller particles tend to have significantly higher surface area for the same particle mass compared to larger particles, thereby offering larger surface area for condensation of toxic volatile organic compounds (VOCs) and PAHs.[38] From measured particulate size–number distribution data, particulate size–surface area distribution can be calculated, assuming all the particles to be spheres (equation (1))

$$dS = dN \cdot \pi D_p^2 \qquad (1)$$

Here, dS is the area distribution, D_p is geometric midpoint diameter of the particle size in a particular channel, and dN is the number concentration of the particulates. This assumption, however, is an oversimplification, therefore it certainly introduces error in the results. It is fairly common to describe the primary exhaust particles as uniform in size with geometries similar to spheres and diameters of roughly 25 nm.[39] Diesel agglomerates consist of primary particles, which are not at all uniform in shape or size, and a common way to quantify this irregularity is by using the fractal dimensions.[40] Irregularity of soot particles affects their environmental impact for several reasons: as particles

become more irregular, their surface area increases, light extinction efficiency increases, aerodynamic behavior changes, filtering efficiency increases, and so on.[40,41]

Figures 10 and 11 show some interesting results, where the distribution for particle surface area per unit volume of exhaust gas is plotted against the particle size for tests conducted at different intake air temperatures and λ for gasoline and n-butanol.

It is observed from Figures 10 and 11 that particle surface area increased as engine was operated using richer mixtures at each intake air temperature for both fuels. Peak surface area concentration of particles depends on the mixture strength (i.e. engine load) and intake air temperature (i.e. combustion phasing) for both fuels. It can also be observed from Figures 10 and 11 that peak surface area distribution of gasoline lies between 6.52×10^{11} and 2.91×10^{12} nm^2/cm^3 at 1200 r/min and 3.60×10^{11} and 5.56×10^{12} nm^2/cm^3 at 2400 r/min. Peak surface area distribution of butanol lies between 1.76×10^{11} and 1.75×10^{12} nm^2/cm^3 at 1200 r/min and 4.71×10^{11} and 6.13×10^{12} nm^2/cm^3 at 2400 r/min. Peak of surface area distribution curve was higher at higher engine speeds for both fuels. Butanol particulates showed higher peak surface area at 2400 r/min compared to baseline gasoline, due to higher particle numbers. However, at 1200 r/min, n-butanol particulates showed lower peak surface area as compared to baseline gasoline, due to higher number concentration of particles near 10 nm size range.

It can also be observed from Figures 10 and 11 that leaner mixtures had the peak of surface area distribution for lower mobility diameters at each intake air temperature for both fuels. It was found that mobility diameters of particulates were in the range of 34–93 nm and 60–80 nm at 1200 and 2400 r/min, respectively, for peak of surface area distribution curve with n-butanol. While baseline gasoline particulates had mobility diameter in the size range of 50–110 nm corresponding to peak of particle surface area distribution at both test
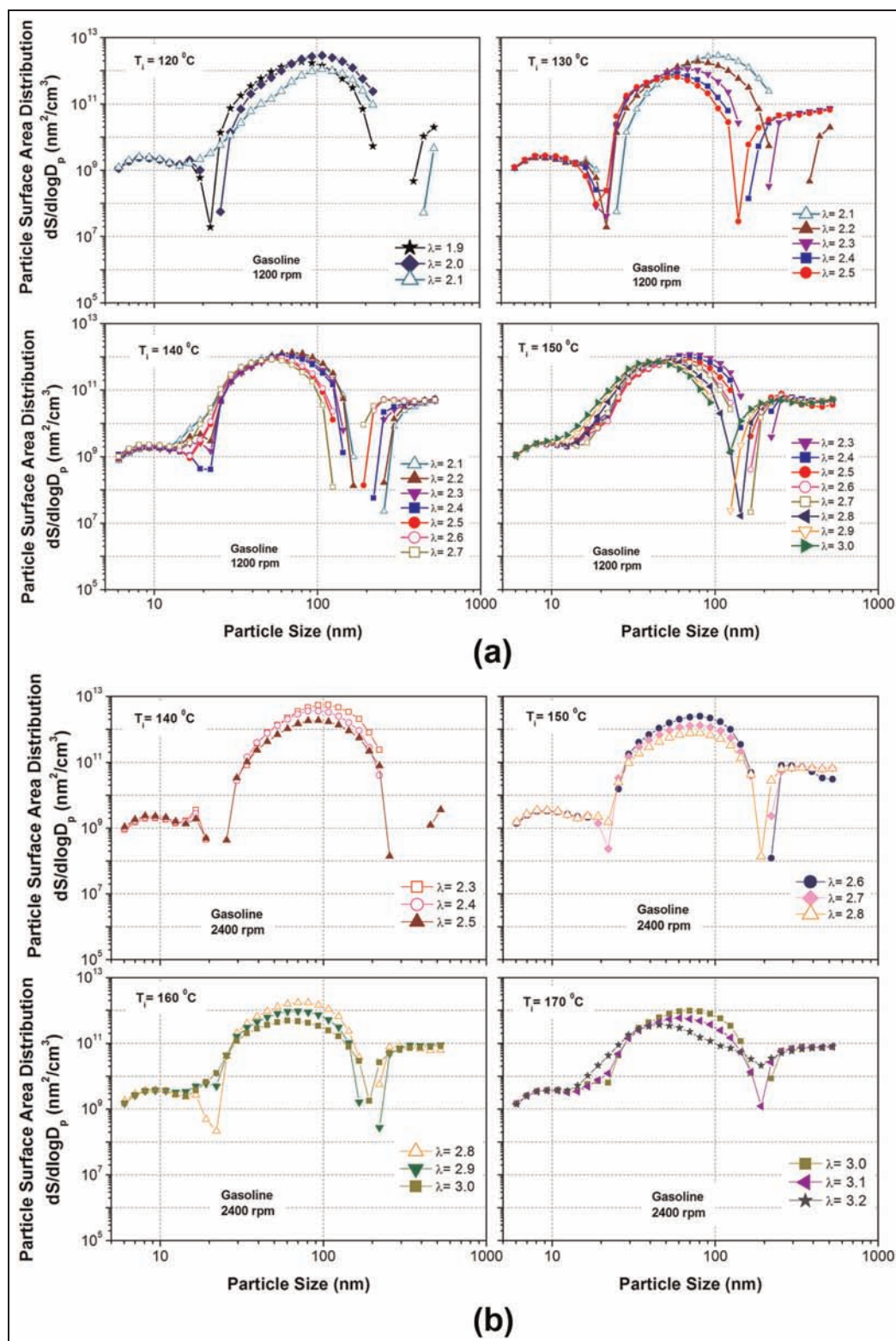
Figure 10. Particulate size–surface area distribution for gasoline HCCI combustion with varying intake temperatures and λ at (a) 1200 and (b) 2400 r/min.

speeds, which were significantly larger than those for n-butanol. Mobility diameters at the peak of surface area distribution curve were larger for both fuels in comparison to mobility diameters corresponding to peak of number concentration curve. This indicates that a large number of significantly larger diameter particulates contribute maximum to the surface area. It can be noted from Figures 10 and 11 that surface area distribution curves in the size range close to 10 nm have number concentration of the order 10^8 nm^2/cm^3 for n-butanol. Gasoline particulates in the size range of 10 nm have number concentration of the order
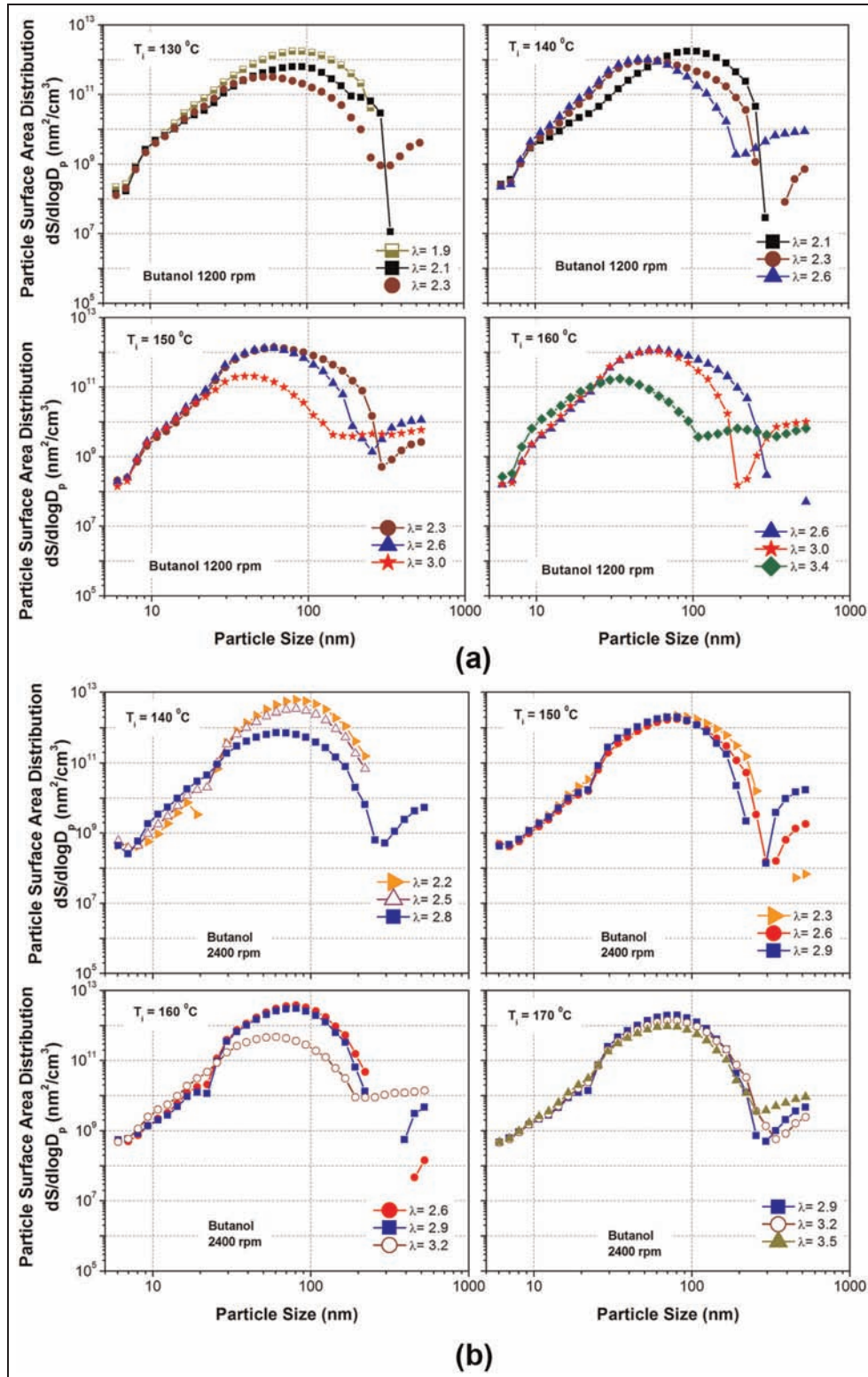
Figure 11. Particulate size–surface area distributions for n-butanol HCCI combustion with varying intake temperatures and λ at (a) 1200 and (b) 2400 r/min.

10^9 nm^2/cm^3, which is an order of magnitude higher as compared to n-butanol (Figures 10 and 11) due to higher particle number concentrations.

The particulate mass versus particle size distribution curve represents the mass of the particles in that particular size range. Since the mass is higher for larger particles, the possibility of their settling down is also higher. The atmospheric retention time for the tiny nanoparticles is higher than larger particles for the same reason. Majority of particulate mass is formed during surface growth stage and agglomeration stage of particulate evolution; thus, the residence time during
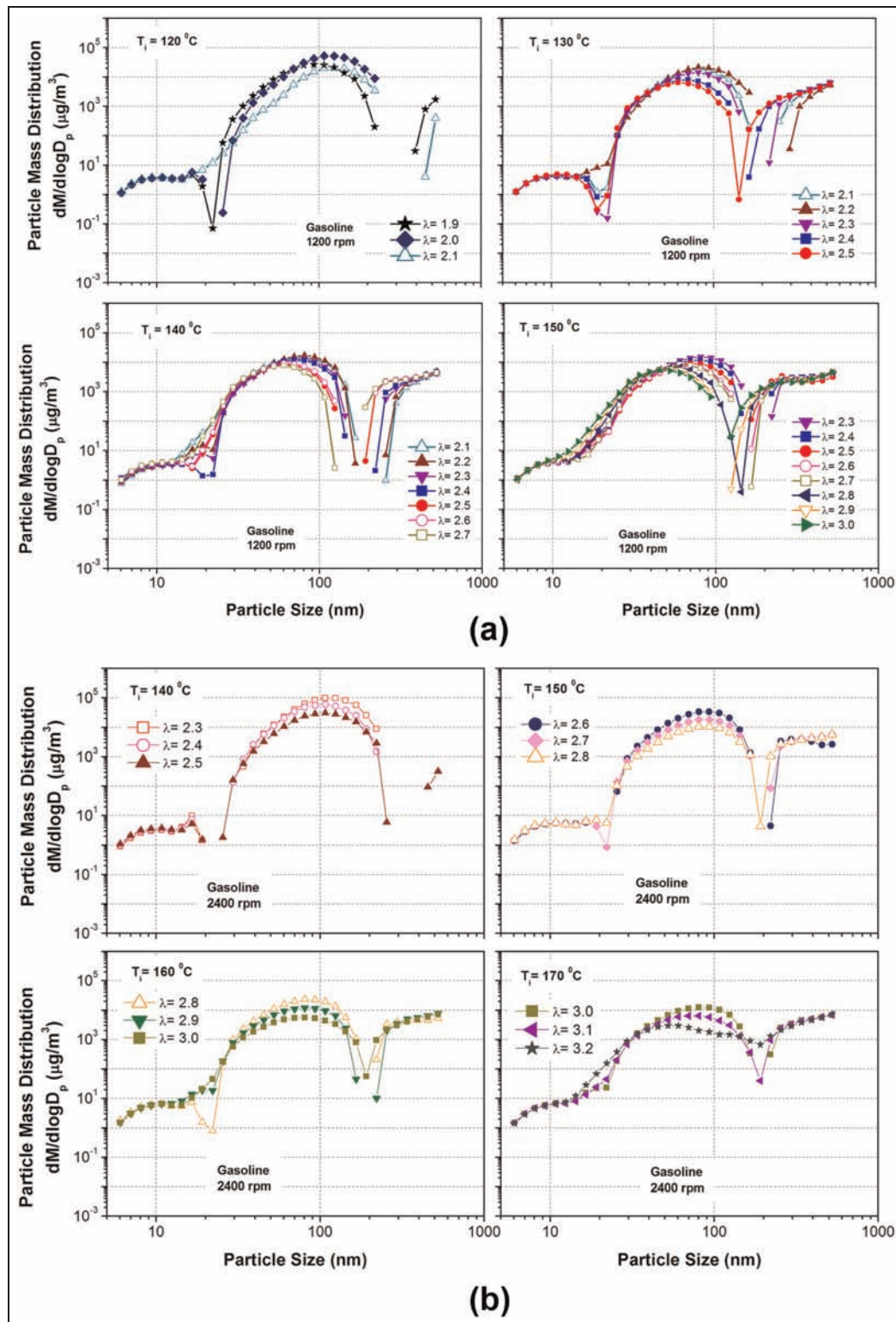
Figure 12. Particle size–mass distributions for gasoline HCCI combustion with varying intake temperatures and λ at (a) 1200 and (b) 2400 r/min.

surface growth process has a large influence on the total particulate mass emissions. Currently, the cumulative mass of particulate emitted by engines is very important from emission legislation point of view. As of today, global automotive emission regulations rely on compliance of mass emissions of particulates and total particulate numbers; however, they do not give any weightage to the size and number distribution, as such. This is a skewed way because the heavier particles are less harmful, and they do contribute to the mass heavily. On the contrary, large number of tiny particles will be more harmful; however, they would not contribute to mass significantly. Therefore, the mass distribution curve of the particulates emitted from an engine
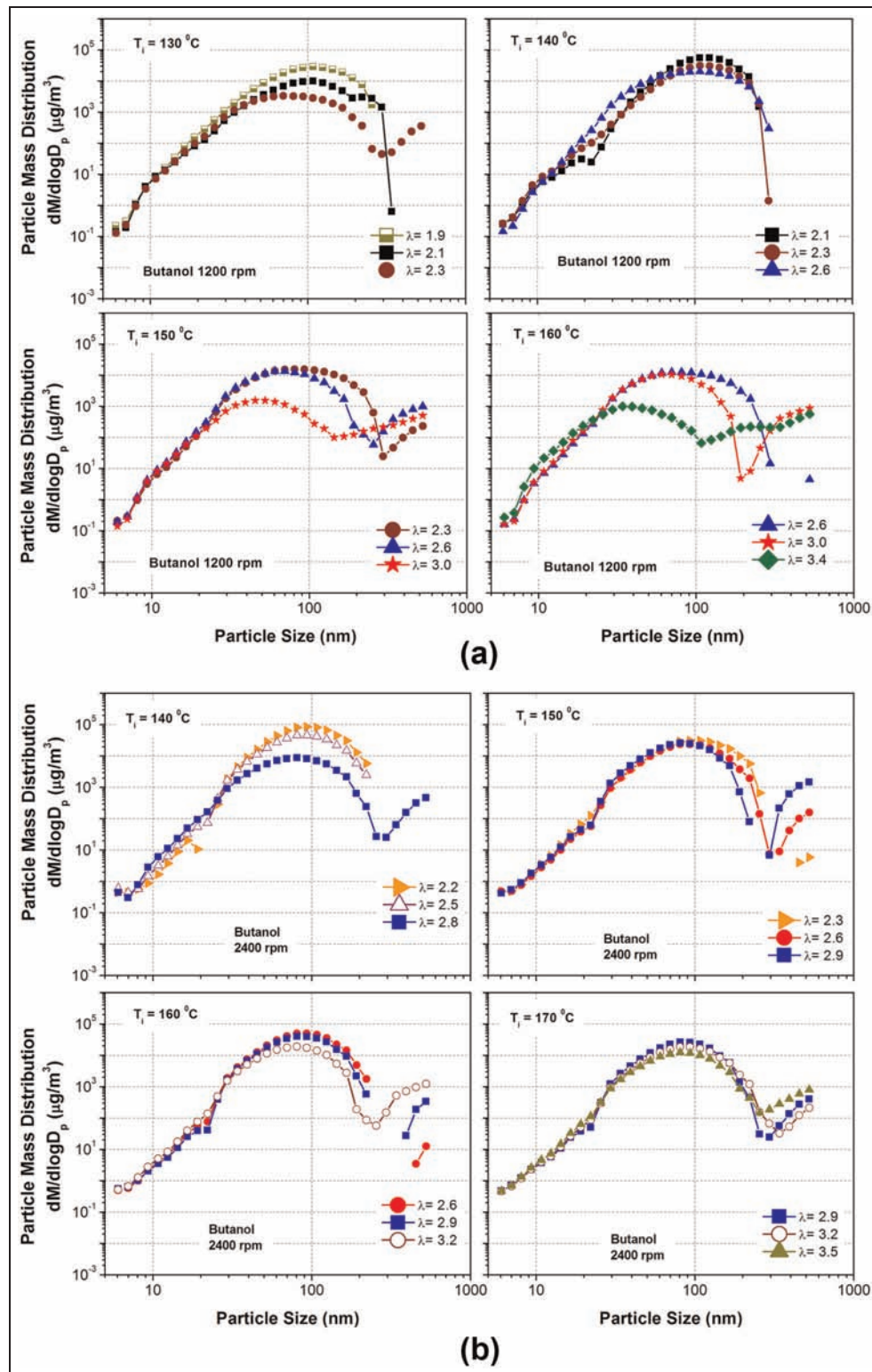
Figure 13. Particle size–mass distributions for n-butanol HCCI combustion with varying intake temperatures and λ at (a) 1200 and (b) 2400 r/min.

will become increasingly important for future emission legislations. With increasing awareness about the harmful effects of nanoparticles on the human health, law makers will be forced to take cognigence of particulate size, surface area, and mass distributions while formulating future emission norms.[38] For all the calculations, a constant particle density of 1.0 g/cm^3 was used in this

investigation. Schneider et al.[42] showed that this particulate density is a reasonable estimate of density for PM originating from engine lubricating oil. This density was also used for PM studies on a gasoline-fueled HCCI engine.[28]

Figures 12 and 13 show particle size–mass distributions from gasoline and n-butanol HCCI engines with

varying intake air temperatures and relative air–fuel ratios (λ) at 1200 and 2400 r/min. Particle mass concentration increased when the engine was operated with richer mixtures at each intake air temperature for both fuels. It was found that particle sizes close to 10 nm had significant number concentration, but their mass concentration was very low as compared to the peak of mass concentration (4–5 orders of magnitude lower). From environmental and human health standpoint, number concentration of the particles is very important and cannot be neglected. It can also be observed from Figures 12 and 13 that leaner mixtures had the peak of mass concentration at lower mobility diameters for both fuels, but this mobility diameter was larger as compared to mobility diameter corresponding to peak number concentration. Peak mass concentration of particles depends on the engine operating conditions such as mixture strength (i.e. engine load) and intake air temperature (i.e. combustion phasing) for both fuels. It can be observed from Figures 12 and 13 that peak mass concentration of gasoline lies between 5.43×10^3 and $5.22 \times 10^4\ \mu g/m^3$ at 1200 r/min and 6.97×10^3 and $9.95 \times 10^4\ \mu g/m^3$ at 2400 r/min. Peak mass concentration of n-butanol was between 9.97×10^2 and $5.58 \times 10^4\ \mu g/m^3$ at 1200 r/min and 8.71×10^3 and $8.65 \times 10^4\ \mu g/m^3$ at 2400 r/min. Maximum peak mass concentration was higher at higher engine speeds for both fuels. Butanol has higher peak mass concentration at 2400 r/min as compared to baseline gasoline, similar to surface area trend. It was also found that mobility diameters were in the range of 52–110 and 80–110 nm at 1200 and 2400 r/min, respectively, for peak mass concentration using n-butanol. While gasoline had mobility diameters in the size range of 45–110 and 80–110 nm corresponding to peak particle mass concentration at 1200 and 2400 r/min, respectively, almost similar to n-butanol. Mobility diameters corresponding to peak mass concentration were larger for both fuels in comparison to mobility diameter corresponding to peak number concentration.

Conclusion

Experiments were conducted on a HCCI combustion engine operating at different inlet air temperatures (T_i) and relative air–fuel ratios at 1200 and 2400 r/min using gasoline and n-butanol with an objective to investigate the effect of engine operating conditions on particulate emissions. It was found that IMEP was mainly affected by λ in HCCI operating region. HCCI operating region decreased with increasing engine speed for both test fuels. Peak particle number concentration increased with increasing mixture strength at each intake air temperature for both fuels. Maximum peak number concentration was higher at higher engine speeds for both fuels. Butanol showed higher peak number concentration at both engine speeds as compared to baseline gasoline. Particle sizes having significant number of particles were in the range of 6–150 nm

in all test conditions. Leaner mixtures had the peak concentration for lower mobility diameters at each intake air temperature for both fuels. It was found that mobility diameters were in the range of 22–52 and 39–60 nm at 1200 and 2400 r/min, respectively, for peak particle number concentration using n-butanol. While baseline gasoline mobility diameters were in the size range of 34–80 nm corresponding to peak particle number concentration at both engine speeds, which was significantly larger than n-butanol. On increasing intake air temperature, mobility diameters corresponding to peak number concentration of particles moved towards lower mobility diameters. Gasoline origin particles in the size range of 10 nm were an order of magnitude higher in number as compared to n-butanol. Total particle number concentration decreased as the fuel-air mixture became leaner and increased with increase in intake air temperature for constant fueling. Maximum value to total number concentration of particles was lower for baseline gasoline as compared to n-butanol for both engine speeds. CMD of particles was in the range of 35–80 and 20–65 nm for gasoline and n-butanol, respectively, for all test conditions in HCCI operating range. Average diameter of particles emitted from butanol was smaller as compared to gasoline. Particle surface area and mass also increased as engine was operated using richer mixtures at each intake air temperature for both fuels. Mobility diameters at the peak of surface area and mass distribution curves were larger for both fuels in comparison to mobility diameters corresponding to peak number concentration curve.

References

1. Kelly-Zion PL and Dec JE. A computational study of the effect of the fuel-type on the ignition time in HCCI engines. *P Combust Inst* 2000; 28(1): 1187–1194.

2. Mack JH, Aceves SM and Dibble RW. Demonstrating direct use of wet ethanol in a homogeneous charge compression ignition (HCCI) engine. *Energy* 2009; 34(6): 782–787.

3. Maurya RK and Agarwal AK. Experimental investigation of the effect of the intake air temperature and mixture quality on the combustion of a methanol and gasoline-fuelled homogeneous charge compression ignition engine. *Proc IMechE, Part D: J Automobile Engineering* 2009; 223(11): 1445–1458.

4. Maurya RK and Agarwal AK. Experimental study of combustion and emission characteristics of ethanol fuelled port injected homogeneous charge compression ignition (HCCI) combustion engine. *Appl Energ* 2011; 88(4): 1169–1180.

5. Maurya RK and Agarwal AK. Experimental investigation of cycle-by-cycle variations in CAI/HCCI combustion of gasoline and methanol fuelled engine. SAE paper 2009-01-1345, 2009.

6. Tongroon M and Zhao H. Combustion characteristics of CAI combustion with alcohol fuels. SAE paper 2010-01-0843, 2010.

7. Maurya RK and Agarwal AK. Experimental investigation of cyclic variations in HCCI combustion parameters for gasoline like fuels using statistical methods. *Appl Energ* 2013; 111: 310–323.

8. Wang H, Reitz RD, Yao M, Yang B, Jiao Q and Qiu L. Development of an n-heptane-n butanol-PAH mechanism and its application for combustion and soot prediction. *Combust Flame* 2013; 160(3): 504–519.

9. Regalbuto C, Pennisi M, Wigg B and Kyritsis D. Experimental investigation of butanol isomer combustion in spark ignition engines. SAE paper 2012-01-1271, 2012.

10. Wigg B, Coverdill R, Lee C and Kyritsis D. Emissions characteristics of neat butanol fuel using a port fuel-injected, spark-ignition engine. SAE paper 2011-01-0902, 2011.

11. Szwaja S and Naber JD. Combustion of n-butanol in a spark-ignition IC engine. *Fuel* 2010; 89: 1573–1582.

12. Rakopoulos DC, Rakopoulos CD, Papagiannakis RG and Kyritsis DC. Combustion heat release analysis of ethanol or n-butanol diesel fuel blends in heavy-duty DI diesel engine. *Fuel* 2011; 90(5): 1855–1867.

13. Rakopoulos CD, Dimaratos AM, Giakoumis EG and Rakopoulos DC. Investigating the emissions during acceleration of a turbocharged diesel engine operating with bio-diesel or n-butanol diesel fuel blends. *Energy* 2010; 35(12): 5173–5184.

14. Rakopoulos DC, Rakopoulos CD, Hountalas DT, Kakaras EC, Giakoumis EG and Papagiannakis RG. Investigation of the performance and emissions of bus engine operating on butanol/diesel fuel blends. *Fuel* 2010; 89: 2781–2790.

15. Rakopoulos DC, Rakopoulos CD, Giakoumis EG, Dimaratos AM and Kyritsis DC. Effects of butanol diesel fuel blends on the performance and emissions of a high-speed DI diesel engine. *Energ Convers Manage* 2010; 51: 1989–1997.

16. Agathou MS and Kyritsis DC. Experimental investigation of bio-butanol laminar non-premixed flamelets. *Appl Energ* 2012; 93: 296–304.

17. Agathou MS and Kyritsis DC. An experimental comparison of non-premixed bio-butanol flames with the corresponding flames of ethanol and methane. *Fuel* 2011; 90(1): 255–262.

18. Liu H, Lee CF, Huo M and Yao M. Combustion characteristics and soot distribution of neat butanol and neat soybean biodiesel. *Energ Fuel* 2011; 25: 3192–3203.

19. Mitsingas CM and Kyritsis DC. Comparison of extinction strain rates of n-butanol and iso-butanol in counter flow non-premixed laminar flamelets. In: *Spring technical meeting of the central states section of the combustion institute*, Ohio, USA, 22–24 April 2012, pp. 343–347. PA, USA: The Combustion Institute.

20. Mitsingas CM and Kyritsis DC. Comparative evaluation of extinction through strain among three alcoholic butanol isomers in non-premixed counterflow flames. *J Energ Eng: ASCE*. Epub ahead of print 19 July 2013. DOI: 10.1061/(ASCE)EY.1943-7897.0000148.

21. Fushimi K, Kinoshita E and Yoshimoto Y. Effect of butanol isomer on diesel combustion characteristics of butanol/gas oil blend. SAE paper 2013-32-9097, 2013.

22. Petrovic VS, Jankovic SP, Tomic MV, Jovanovic ZS and Dragan K. The possibilities for measurement and characterization of diesel engine fine particles—a review. *Therm Sci* 2011; 15(4): 915–938.

23. Dorie LD, Bagley ST, Leddy DG and Johnson JH. Characterization of mutagenic subfractions of diesel exhaust modified by ceramic particulate traps. *Environ Sci Technol* 1987; 21(8): 757–765.

24. Price P, Stone R, Misztal J, Xu H, Wyszynski M, Wilson T and Qiao J. Particulate emissions from a gasoline homogeneous charge compression ignition engine. SAE paper 2007-01-0209, 2007.

25. Kittelson DB and Franklin L. Nanoparticle emissions from an ethanol fuelled HCCI engine. In: *Cambridge particle meeting 2010*, Cambridge, UK, 21 May 2010. Cambridge, UK: Cambridge Particle Meeting, University of Cambridge's Department of Engineering.

26. Maurya RK and Agarwal AK. Effect of start of injection on the particulate emission from methanol fuelled HCCI engine. *SAE Int J Fuels Lubr* 2011; 4(2): 204–222.

27. Misztal J, Xu H, Tsolakis A, Wyszynski ML, Constandinides G, Price P and Qiao J. Influence of inlet air temperature on gasoline HCCI particulate emissions. *Combust Sci Technol* 2009; 181(5): 695–709.

28. Misztal J, Xu H, Wyszynski ML, Price P, Stone R and Qiao J. Effect of injection timing on gasoline homogeneous charge compression ignition particulate emissions. *Int J Engine Res* 2009; 10(6): 419–430.

29. Agarwal AK, Singh AP, Lukose J and Gupta T. Characterization of exhaust particulates from diesel fuelled homogenous charge compression ignition combustion engine. *J Aerosol Sci* 2013; 58: 71–85.

30. TSI. Operation and service manual, Engine Exhaust Particle Sizer™ Spectrometer Model 3090. March 2009.

31. Johansson T, Borgqvist P, Johansson B, Tunestål P and Aulin H. HCCI heat release data for combustion simulation, based on results from a turbocharged multi cylinder engine. SAE paper 2010-01-1490, 2010.

32. Johansson T, Johansson B, Tunestål P and Aulin H. HCCI operating range in a turbo-charged multi cylinder engine with VVT and spray-guided DI. SAE paper 2009-01-0494, 2009.

33. Gupta T, Kothari A, Srivastava DK and Agarwal AK. Measurement of number and size distribution of particles emitted from a mid-sized transportation multipoint port fuel injection gasoline engine. *Fuel* 2010; 89(9): 2230–2233.

34. Franklin L. *Effects of homogeneous charge compression ignition (HCCI) control strategies on particulate emissions of ethanol fuel*. PhD Thesis, University of Minnesota, Minneapolis, MN, 2010 (December).

35. Tobias HJ, Beving DE, Ziemann PJ, Sakurai H, Zuk M, McMurry PH, et al. Chemical analysis of diesel engine nanoparticles using a nano-DMA-thermal desorption particle beam mass spectrometer. *Environ Sci Technol* 2001; 35(11): 2233–2243.

36. Sakurai H, Tobias HJ, Park K, Zarling D, Docherty KS, Kittelson DB, et al. On-line measurements of diesel nanoparticle composition and volatility. *Atmos Environ* 2003; 37(9–10): 1199–1210.

37. Miller AL, Stipe CB, Habjan MC and Ahlstrand GG. Role of lubrication oil in particulate emissions from a hydrogen-powered internal combustion engine. *Environ Sci Technol* 2007; 41(19): 6828–6835.

38. Maurya RK, Srivastava DK and Agarwal AK. Experimental investigations of particulate emitted by an alcohol-fuelled HCCI/CAI combustion engine. *Int Energ J* 2011; 12(1): 29–38.

39. Wentzel M, Gorzawski H, Naumann KH, Saathoff H and Weinbruch S. Transmission electron microscopical and aerosol dynamical characterization of soot aerosols. *J Aerosol Sci* 2003; 34(10): 1347–1370.

40. Lapuerta M, Ballesteros R and Martos FJ. A method to determine the fractal dimension of diesel soot agglomerates. *J Colloid Interf Sci* 2006; 303: 149–158.

41. Kittelson DB. Engines and nanoparticles: a review. *J Aerosol Sci* 1998; 29(1): 575–588.

42. Schneider J, Hock N, Weimer S, Borrmann S, Kirchner U, Vogt R and Scheer V. Nucleation particles in diesel exhaust: composition inferred from in situ mass spectrometric analysis. *Environ Sci Technol* 2005; 39(16): 6153–6161.